

Study of Quasi-Elastic (anti)neutrino interactions in the NOMAD experiment

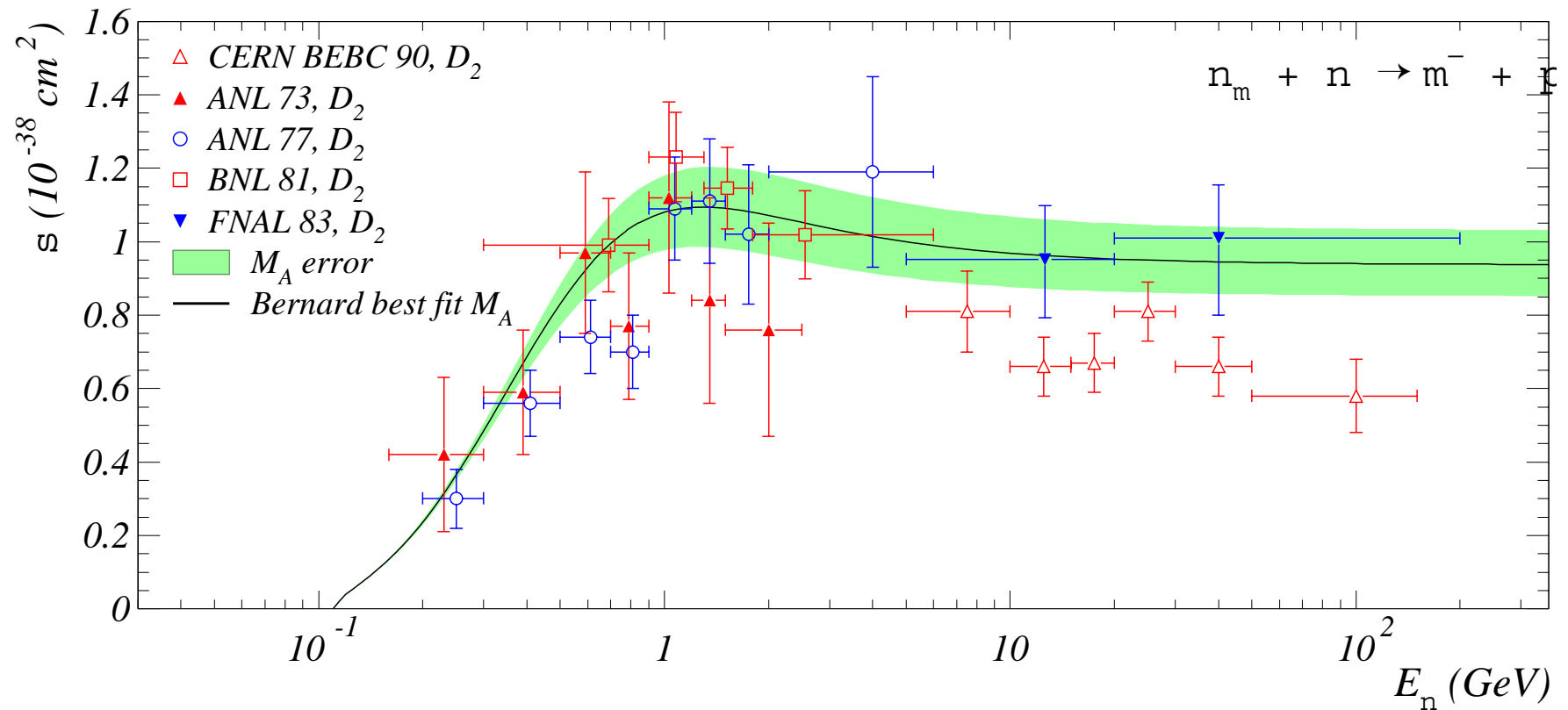


Vladimir Lyubushkin

Joint Institute for Nuclear Research, DLNP, Dubna

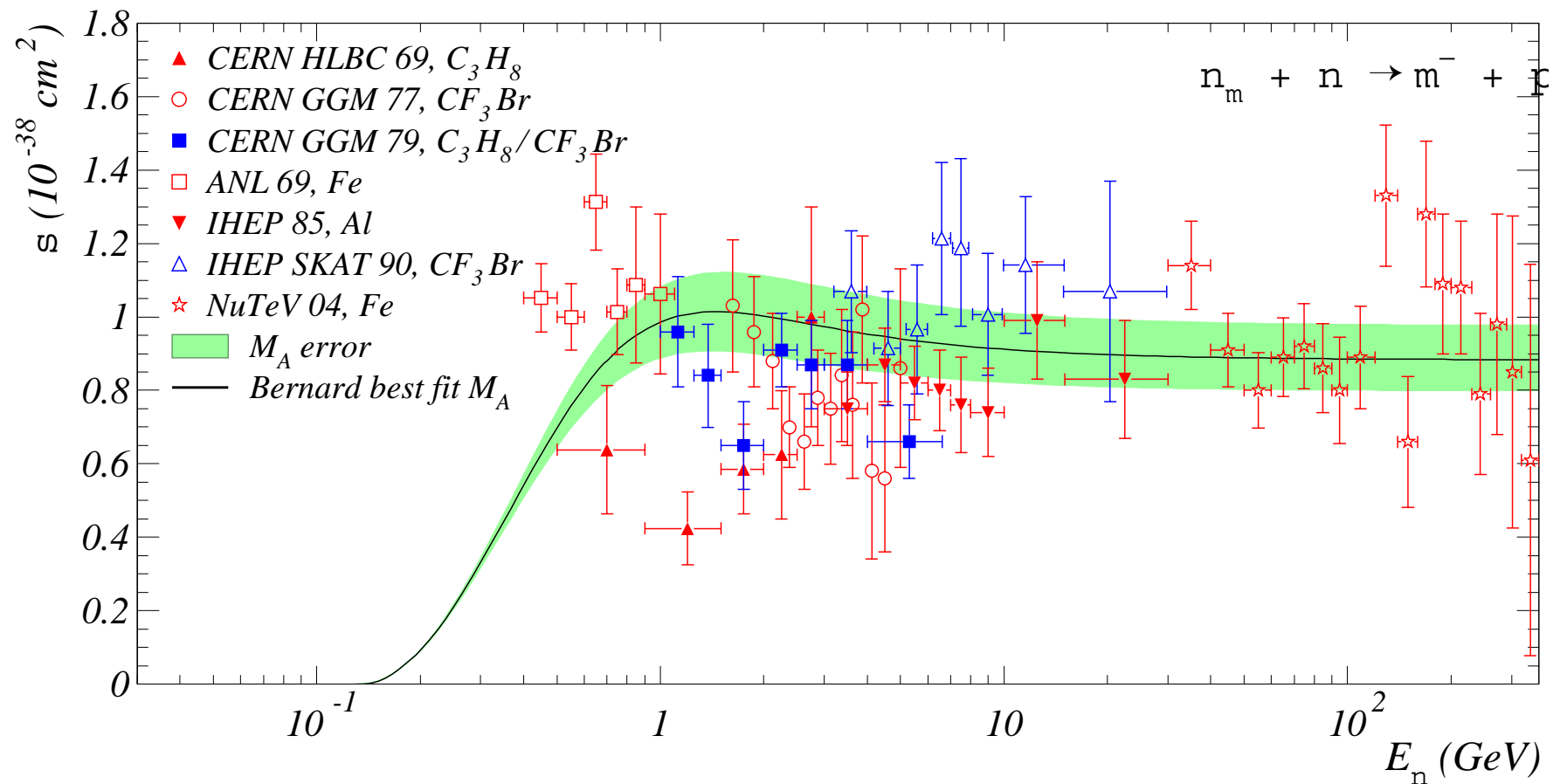
- Review of existing experimental data: total cross-sections and the axial form-factor of the nucleon
- Phenomenology of $\nu_\mu n \rightarrow \mu^- p$ and $\bar{\nu}_\mu p \rightarrow \mu^+ n$ processes: MC simulation and nuclear reinteraction (FSI) effects
- Description of the NOMAD detector
- Selection of quasi-elastic events in NOMAD: topology and kinematic criteria
- The QEL cross section measurement and the axial mass M_A extraction from Q^2 distribution
- Our **results** and **conclusions**

Total QE $\nu_\mu n$ cross section from deuterium filled bubble chambers



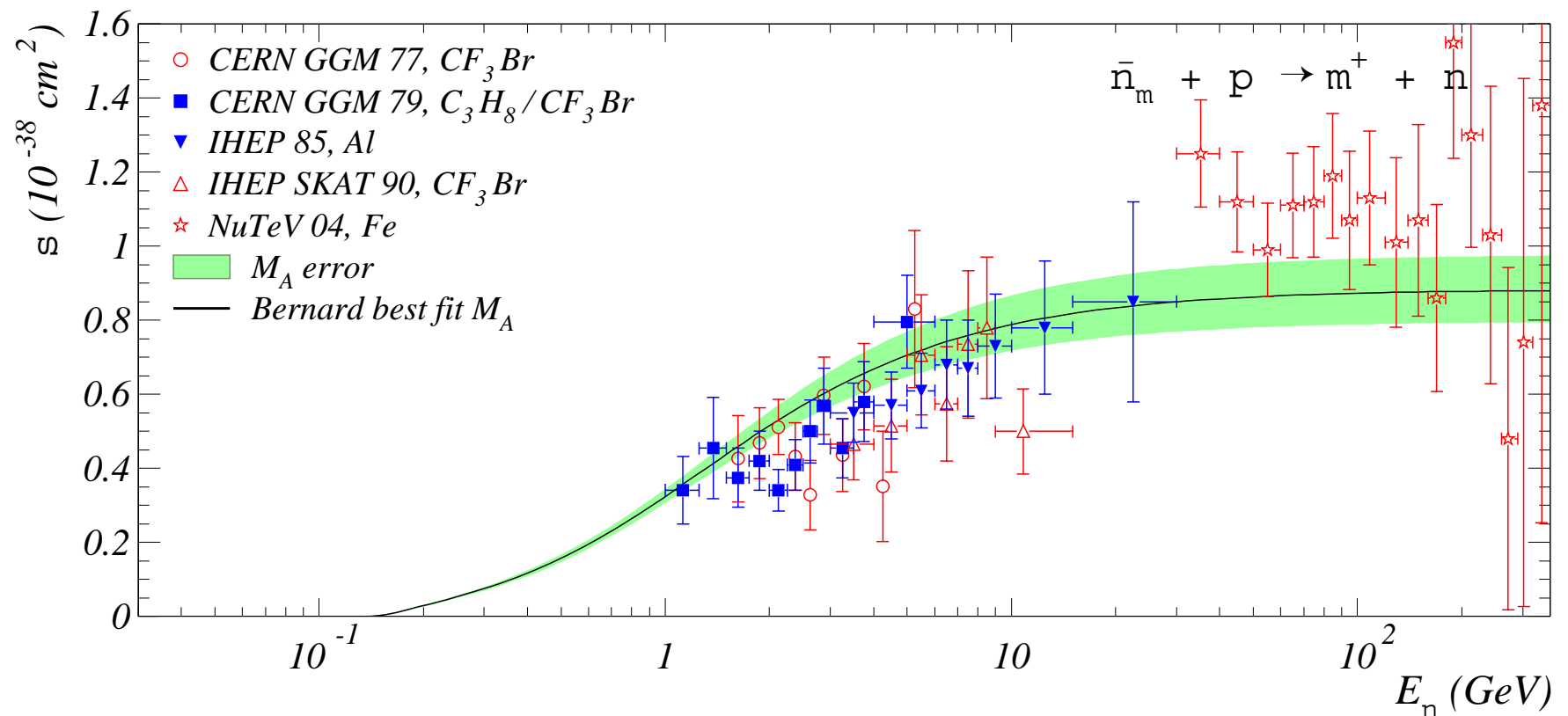
The total cross-section of $\nu_\mu n \rightarrow \mu^- p$ process extracted from $\nu_\mu D$ scattering data. The solid curve corresponds to the world average value of axial mass $M_A = 1.03$ GeV while the shaded area shows a ± 0.1 GeV error band. Points correspond to available experimental data from ANL (Argonne 12-foot BC), BNL (Brookhaven 7-foot BC), FNAL (FermiLab 15-foot BC), CERN (BEBC, Big European Bubble Chamber). **Corrections for nuclear effects have been made by the authors of the experiments.**

Total QE $\nu_\mu n$ cross section measured on heavy nuclei target



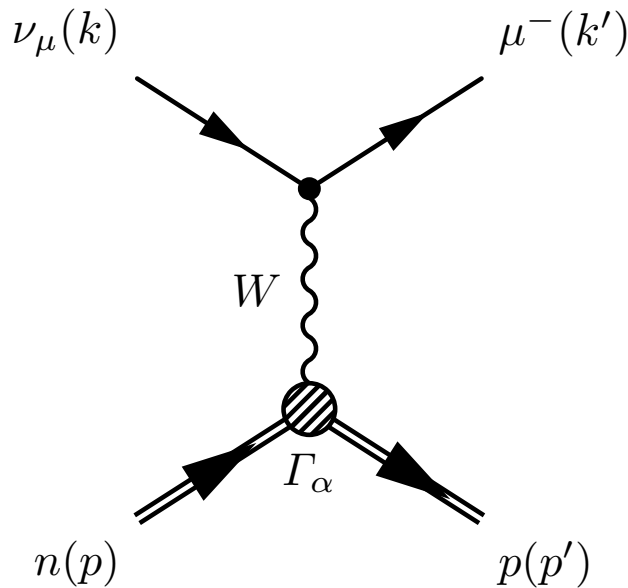
The total cross-section of $\nu_\mu n \rightarrow \mu^- p$ process extracted from the data on ν_μ scattering off heavy nuclei. Nuclear effects are included into calculations according to the relativistic Fermi gas model by Smith and Moniz for Carbon with binding energy $E_b = 25.6$ MeV and Fermi momentum $P_F = 221$ MeV; the axial mass value is $M_A = 1.03 \pm 0.1$ GeV. Points correspond to available experimental data from ANL (Spark-chamber), NuTeV (FermiLab), CERN (Heavy Liquid Bubble Chamber, Gargamelle BC), IHEP (Spark-chamber and SCAT BC).

Total QE cross $\bar{\nu}_\mu p$ cross section measured on heavy nuclei target



The total cross-section of $\bar{\nu}_\mu p \rightarrow \mu^+ n$ process extracted from the data on $\bar{\nu}_\mu$ scattering off heavy nuclei. Nuclear effects are included into calculations according to the relativistic Fermi gas model by Smith and Moni for Carbon; the axial mass value is $M_A = 1.03 \pm 0.1$ GeV. Points correspond to available experimental data from NuTeV, CERN (Gargamelle BC), IHEP (Spark-chamber and SCAT BC).

Phenomenology of Quasi-Elastic Neutrino Scattering



The most general form of the electroweak $N_{in} \rightarrow N_{out}$ transition current is given by ^a

$$J_\alpha = \langle N_{out}; p' | \hat{J}_\alpha | N_{in}; p \rangle = \bar{u}_p(p') \Gamma_\alpha u_n(p)$$

Here p and p' are the 4-momenta of the target nucleon N_{in} and final baryon N_{out} respectively. The the vertex 4-vector is

$$\Gamma_\alpha = \gamma_\alpha F_1 + i\sigma_{\alpha\beta} \frac{q^\beta}{2M} F_2 + \frac{q_\alpha}{M} F_S + \left(\gamma_\alpha F_A + \frac{p_\alpha + p'_\alpha}{M} F_T + \frac{q_\alpha}{M} F_P \right) \gamma_5$$

The six form factors $F_i(Q^2)$ in the vertex function Γ_α are in general complex.

The most general restrictions to the form factors:

1. T invariance $\implies \text{Im}(F_V, F_M, F_A, F_P, F_S, F_T) = 0$;
2. C invariance $\implies \text{Im}(F_V, F_M, F_A, F_P) = 0$ and $\text{Re}(F_S, F_T) = 0$;
3. no SCC $\implies F_S = F_T = 0$ ($\equiv T$ invariance + C invariance);
4. $\partial_\alpha V^\alpha = 0$ (CVC) $\implies F_S = 0$.

^aC. H. Llewellyn Smith, "Neutrino reactions at accelerator energies," Phys. Rept. 3 C (1972) 261–379.

Electromagnetic form factors

We have investigated several models for the nucleon electromagnetic Sachs form factors

$$G_E(Q^2) = F_1(Q^2) - \frac{Q^2}{4M_i^2} F_2(Q^2) \quad \text{and} \quad G_M(Q^2) = F_1(Q^2) + F_2(Q^2)$$

where $F_1(Q^2)$ and $F_2(Q^2)$ are the Dirac and Pauli form factors, respectively.

- ❖ Simple dipole parametrization:

$$G_E(Q^2) = G_M(Q^2) / (\mu_p - \mu_n) = G_D(Q^2) = (1 + Q^2/0.71)^{-2}$$

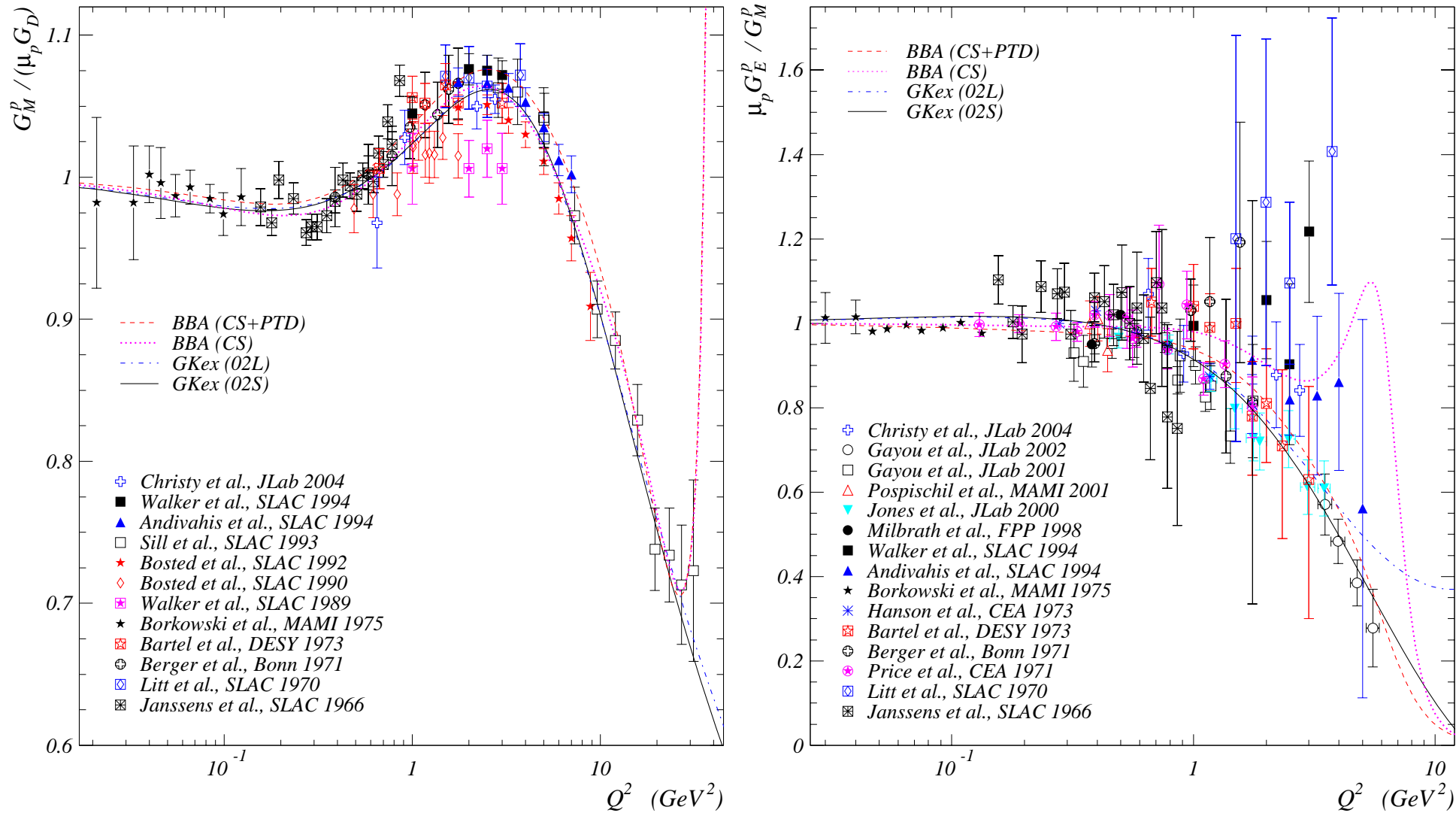
- ❖ Gari–Krüempelmann (GK) model^a extended and fine-tuned by Lomon^b to match current experimental data. Specifically, as the “reference model”, we explore the so-called GKex(02S) which fits the modern and consistent older data well and meets the requirements of dispersion relations and of QCD at low and high 4-momentum transfer.
- ❖ Global fit by Budd *et al.*,^c (BBA model) to the data from Rosenbluth analysis of elastic ep cross section measurements and those from the polarization transfer techniques.

^aM. F. Gari and W. Krüempelmann, “The electric neutron form factor and the strange quark content of the nucleon,” Phys. Lett. B **274** (1992) 159-162; erratum – *ibid.* **282** (1992) 483-484.

^bE. L. Lomon, “Effect of recent R_p and R_n measurements on extended Gari–Krüempelmann model fits to nucleon electromagnetic form factors,” Phys. Rev. C **66** (2002) 045501 [nucl-th/0203081].

^cH. Budd, A. Bodek, and J. Arrington, “Modeling quasi-elastic form factors for electron and neutrino scattering,” hep-ex/0308005, to be published in Nucl. Phys. B (Proc. Suppl.).

Proton electromagnetic form factors

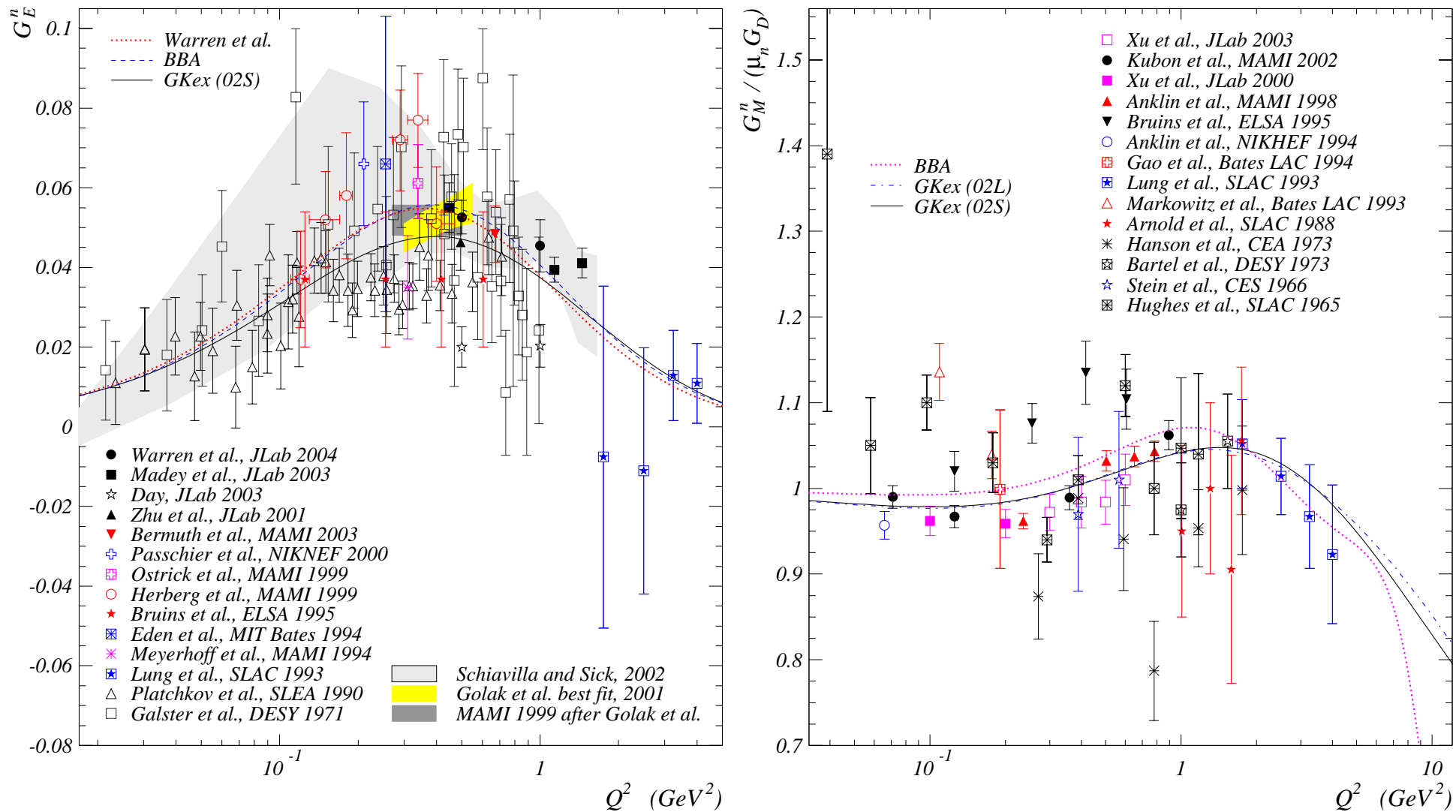


Normalized magnetic form factor and ratio of electric and magnetic form factors of the proton.

BBA: Budd-Bodek-Arrington [hep-ex/0308005] global fit to the data from Rosenbluth analysis of elastic ep cross section measurements and those from the polarization transfer techniques.

GKex: extended Gari-Krüempelmann model after Lomon [PRC **66** (2002) 045501].

Neutron electromagnetic form factors



Electric and normalized magnetic form factors of the neutron. Together with the **BBA** and **GKex** fits (see previous slide), the recent fit by Warren *et al.* [PRL **92** (2004) 042301] is also shown. The filled areas represent some theoretical extractions from different data subsets.

Axial and pseudoscalar form factors

The customary parametrizations for the axial and pseudoscalar form factors are

$$F_A(q^2) = F_A(0) \left(1 - \frac{q^2}{M_A^2}\right)^{-n} \quad \text{with} \quad n = \begin{cases} 2 & \text{("dipole")}, \\ 1 & \text{("monopole")}; \end{cases}$$

$$F_P(q^2) = \frac{2M^2}{m_\pi^2 - q^2} F_A(q^2) \quad (\text{PCAC}) \quad \text{and} \quad F_A(0) = g_A = -1.2695 \pm 0.0029.$$

The pseudoscalar contribution is important for τ production.^a Note that the "standard" expression for the F_P is at most a (doubtful) parametrization inspired by the PCAC hypothesis (+ pion pole dominance near $q^2 = 0$).

The experiments on QE and pion electroproduction permit very wide spread of M_A :

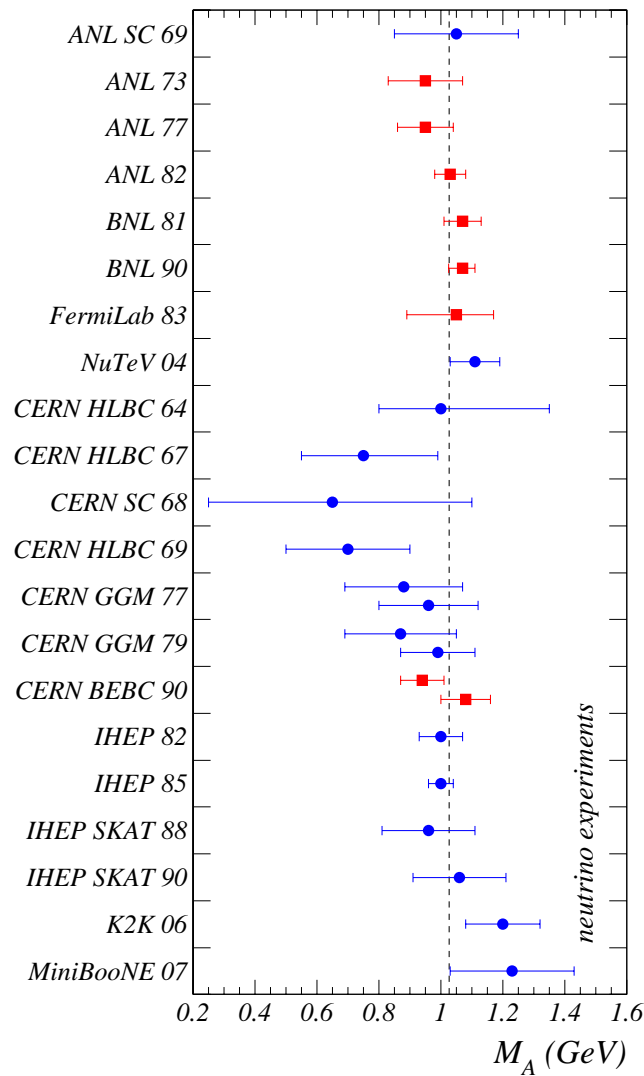
from roughly 0.7 to 1.2 GeV/ c^2 for dipole F_A ,

from roughly 0.6 to 0.8 GeV/ c^2 for monopole F_A .

However the monopole parametrization seems to be obsolete.

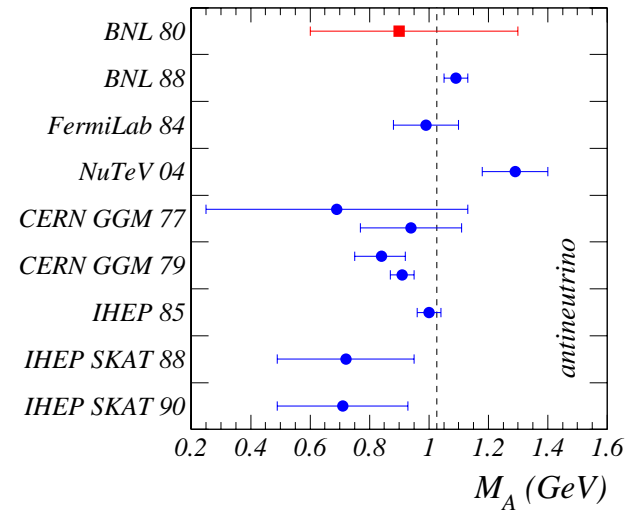
^aK. Hagiwara, K. Mawatari and H. Yokoya, "Pseudoscalar form factors in tau-neutrino nucleon scattering," hep-ph/0403076; see also poster by H. Yokoya in this workshop.

Axial mass from neutrino scattering experiments



- Deuterium filled bubble chambers
- Heavy liquid bubble chambers and spark chambers

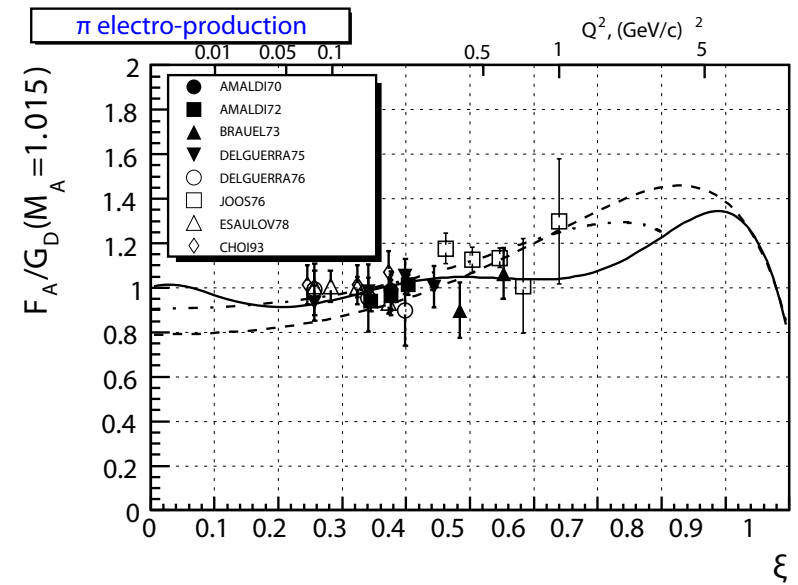
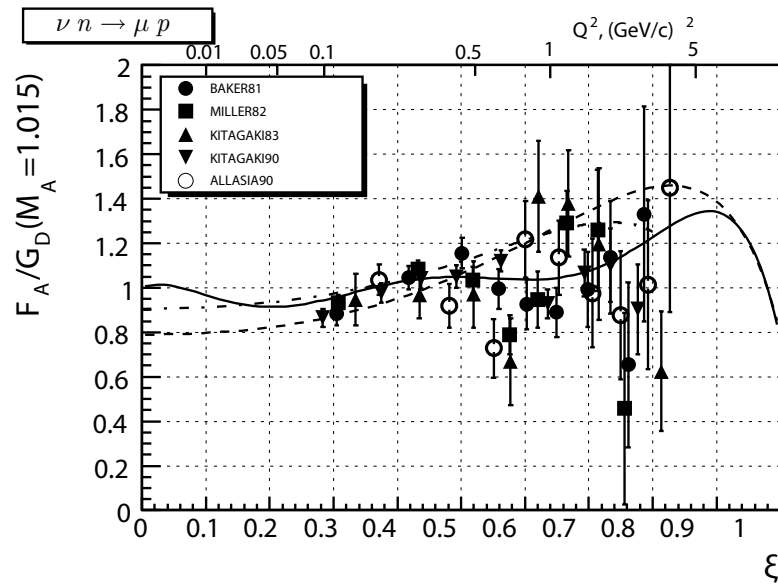
--- M_A world average value



Axial mass average value $M_A = 1.026 \pm 0.021$ GeV was borrowed from review by V. Bernard *et al.*^a

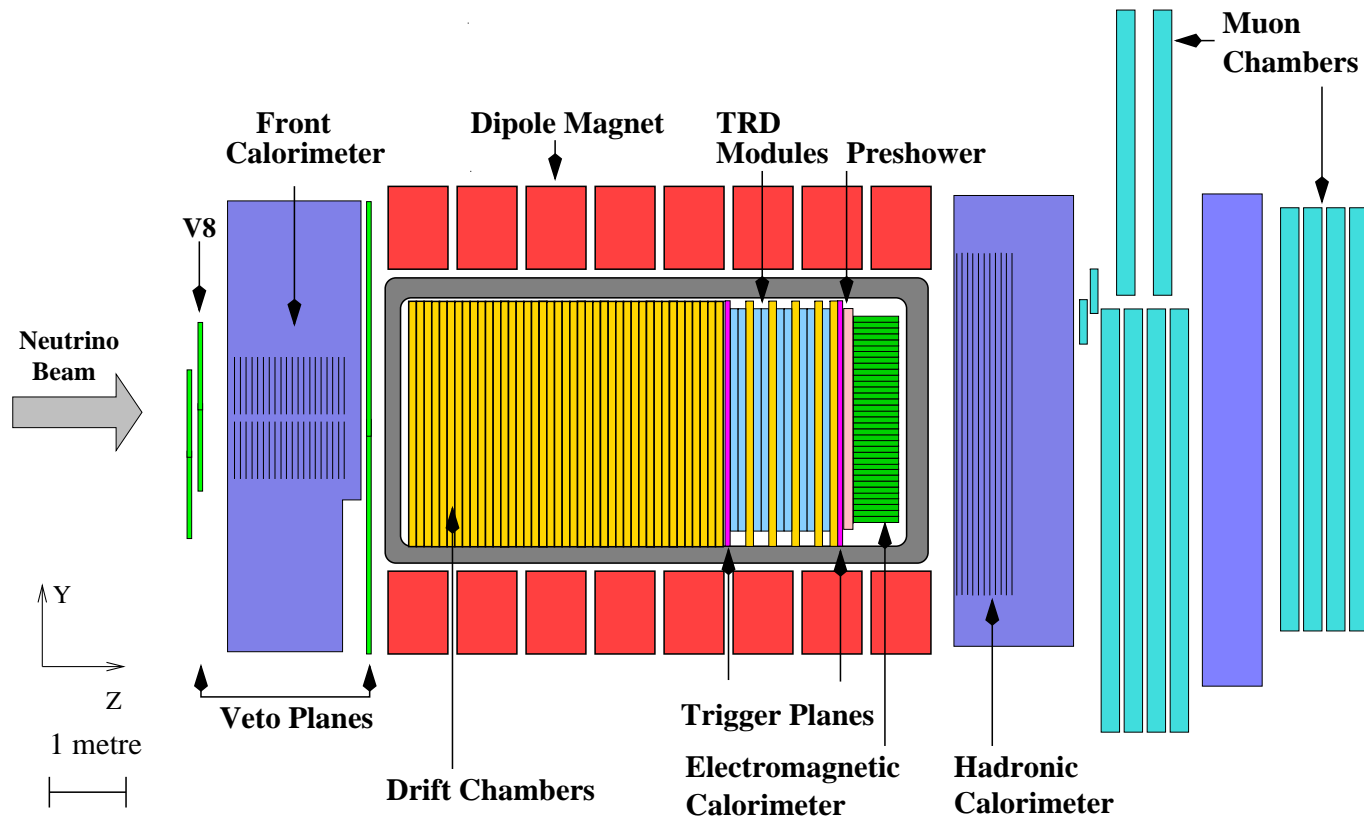
^aV. Bernard, L. Elouadrhiri and Ulf-G. Meißner, "Axial structure of the nucleon," J. Phys. G **28** (2002) R1–R35 [hep-ph/0107088].

Axial form factor from neutrino scattering experiments



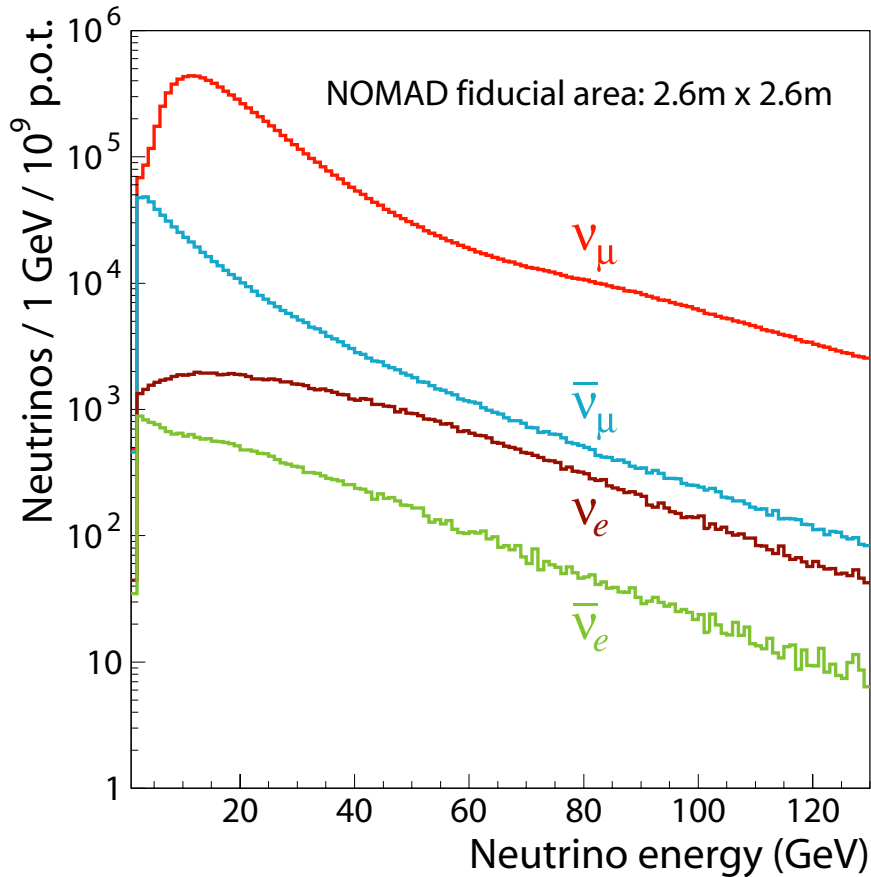
Axial form factor of the nucleon F_A , re-extracted from neutrino-deuteron (left) and pion electroproduction (right) data. Taken from A. Bodek et al, ArXiv: hep-ex/0709.3538.v1

NOMAD experiment



- **Drift Chambers** (target and momentum measurement) Position resolution $< 200 \mu\text{m}$ (small angle tracks)
Momentum resolution $\sim 3.5\%$ ($p < 10 \text{ GeV}/c$)
- **Transition Radiation Detector** for e^\pm identification: π rejection $\sim 10^3$ for electron efficiency $\geq 90\%$
- Lead glass **Electromagnetic Calorimeter** $\frac{\sigma(E)}{E} = (1.04 \pm 0.01)\% + \frac{(3.22 \pm 0.07)\%}{\sqrt{E(\text{GeV})}}$
- **Muon Chambers** for μ^\pm identification: efficiency $\approx 97\%$ ($p_\mu > 5 \text{ GeV}/c$)
- **Hadronic Calorimeter** for n and K_L^0 veto

Neutrino fluxes at NOMAD experiment



ν_x / ν_μ	$\langle E_\nu \rangle, \text{GeV}$
1.0	24.3
0.068	17.2
0.010	36.4
0.0027	27.6

$$\langle \sigma_i \rangle = \int \sigma_i(E_\nu) f(E_\nu) dE_\nu$$

Mode	Neutrino	Antineutrino
QEL	0.430	0.393
RES	0.575	0.430
DIS	15.954	4.834

^aP. Astier *et al.* [NOMAD Collaboration], "Prediction of neutrino fluxes in the NOMAD experiment," Nucl. Instrum. Meth. A **515**, 800 (2003) [arXiv:hep-ex/0306022].

Monte Carlo simulation

- Quasi-elastic neutrino scattering
 - ✓ based on the Llewellyn Smith's formalism ^a
 - ✓ Pauli blocking for outgoing nucleon and impact of nuclear reinteractions in nuclei are taken into account
- Single pion production via intermediate resonance state
 - ✓ based on Rein–Sehgal model ^b
 - ✓ set of 18th baryon resonances with masses below 2 GeV as in RS but with all relevant parameters updated according to the most recent PDG
 - ✓ factors which were estimated in RS numerically are corrected by using the new data and a more accurate integration algorithm
- Deep inelastic scattering
 - ✓ modelled with the help of modified LEPTO 6.1 package ^c
 - ✓ production of all zoo of hadrons is simulated with help of JETSET 7.4 ^d
 - ✓ specific nuclear effects (such as nuclear shadowing, pion excess and off-shell corrections to bound nucleon structure functions) are described in the unique theoretical framework, proposed recently by S. Kulagin and R. Petti ^e

^aC. H. Llewellyn Smith, “Neutrino reactions at accelerator energies,” Phys. Rept. **3 C** (1972) 261–379.

^bD. Rein and L. Sehgal, “Neutrino excitation of baryon resonances and single pion production,” Annals Phys. **133** (1981) 79–153

^cG. Ingelman, LEPTO version 6.1, “The Lund Monte Carlo for Deep Inelastic Lepton-Nucleon Scattering,” TSL-ISV-92-0065 (1992); see also G. Ingelman, A. Edin, J. Rathsman, LEPTO version 6.5, Comp. Phys. Comm. **101** (1997) 108, [hep-ph/9605286]

^dT. Sjöstrand, “PYTHIA 5.7 and JETSET 7.4: physics and manual,” LU-TP-95-20 (1995), [hep-ph/9508391]

^eS. Kulagin, R. Petti, “Global study of nuclear structure functions,” Nucl. Phys. A **765** (2006) 126, [hep-ph/0412425]

Final State Interactions: Intra-nuclear cascade

The simulation of the re-interaction between particles, produced at the primary neutrino collision off the target nucleon, and the residual nucleus has been done with the help of **DPMJET package**^a according to the Formation Zone Intranuclear Cascade model. Secondaries from this first collision are followed along straight trajectories and may also induce in turn intranuclear cascade processes if they reach the end of their formation zone inside the target, otherwise they leave the nucleus without interaction.

There are two important parameters in DPMJet:

- **Formation time** τ_0 controls the development of the intranuclear cascade. With increasing τ_0 the number of cascade generations and the number of low-energy particles will be reduced. Its default value is $\tau_0 = 2.0$.
- **Correction factor** α_{mod}^F . Inside DPMJet the momenta of the spectator nucleons are sampled from the zero temperature Fermi-distribution. However, the nuclear surface effects and the interaction between nucleons result in the reduction of the Fermi momentum. Its default value is $\alpha_{mod}^F = 0.6$.

At the end of intranuclear cascade the residual nucleus is supposed to go through some de-excitation mechanisms. As a result, it can disassemble into two or more fragments, emit photons, nucleons or light particles (like d , α , ${}^3\text{H}$, ${}^3\text{He}$).

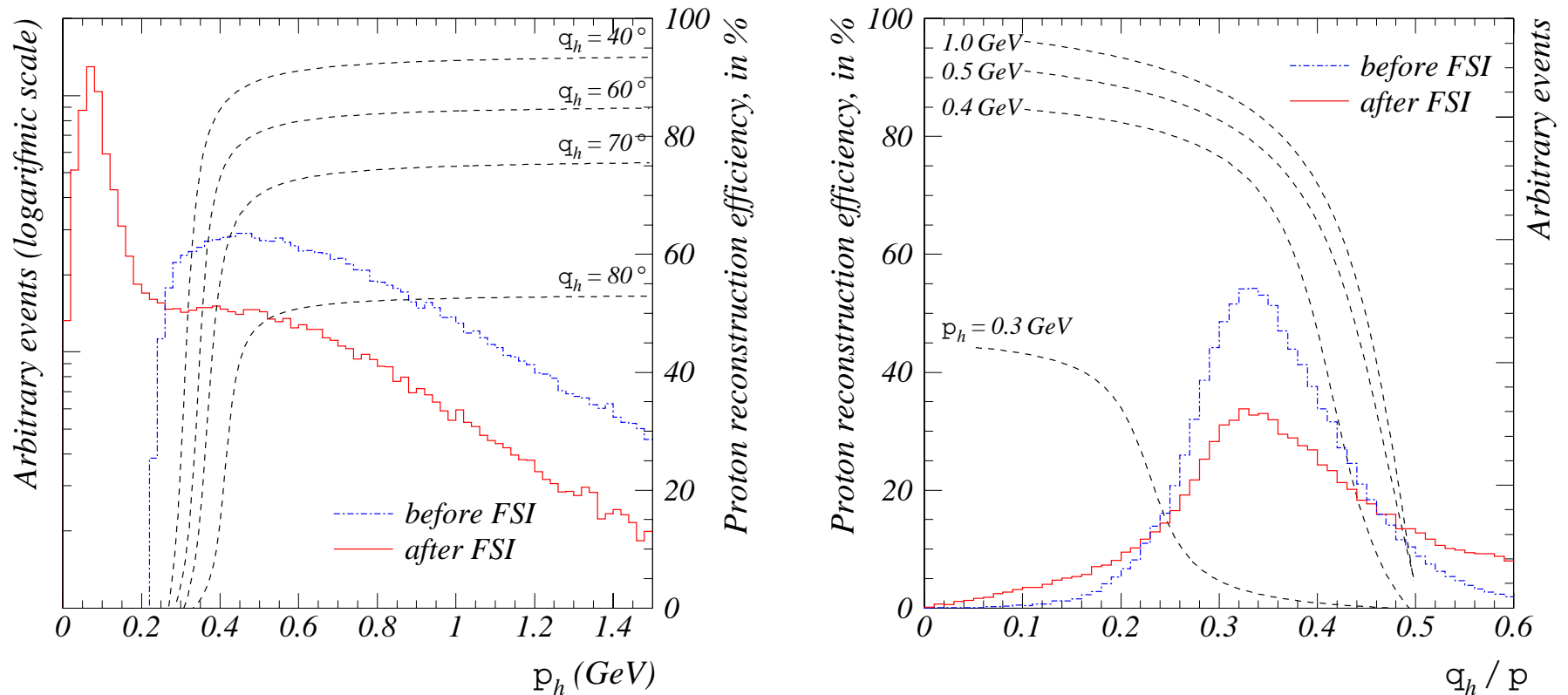
As a cross-check we compare our MC simulation for QEL process with predictions of **NUANCE** event generator^b

The program uses a model of the final state interaction in the nucleus originally developed for the IMB experiment. Hadrons are tracked through the nucleus in 0.2 fm steps, treating the nucleus as an isoscalar sphere of nuclear matter with radially-dependent density and Fermi momentum.

^aJ. Ranft, "DPMJET version II.5: Sampling of hadron hadron, hadron nucleus and nucleus nucleus interactions at accelerator and cosmic ray energies according to the two-component dual parton model: Code manual," arXiv:hep-ph/9911232.

^bD. Casper, "The nuance neutrino physics simulation, and the future," Nucl. Phys. Proc. Suppl. **112**, 161 (2002) [arXiv:hep-ph/0208030].

Intranuclear cascade and proton track reconstruction probability



Distribution of leading proton momentum p_h and emission angle θ_h before (dash-dotted line) and after (solid line) intra-nuclear cascade. Dashed lines show the reconstruction probability of proton track.

QEL cross section measurement: Normalization to Deep Inelastic Scattering

$$\langle \sigma_{qel} \rangle = \langle \sigma_0 \rangle \frac{N_{qel}}{N_0} \quad \Rightarrow \quad \langle \sigma_{qel} \rangle = \frac{1}{\varepsilon_{qel}} \left[\langle \sigma_0 \rangle \frac{N_{dat}}{N_0} - \langle \sigma_{dis} \rangle \varepsilon_{dis} - \langle \sigma_{res} \rangle \varepsilon_{res} \right]$$

Selection of *DIS* events:

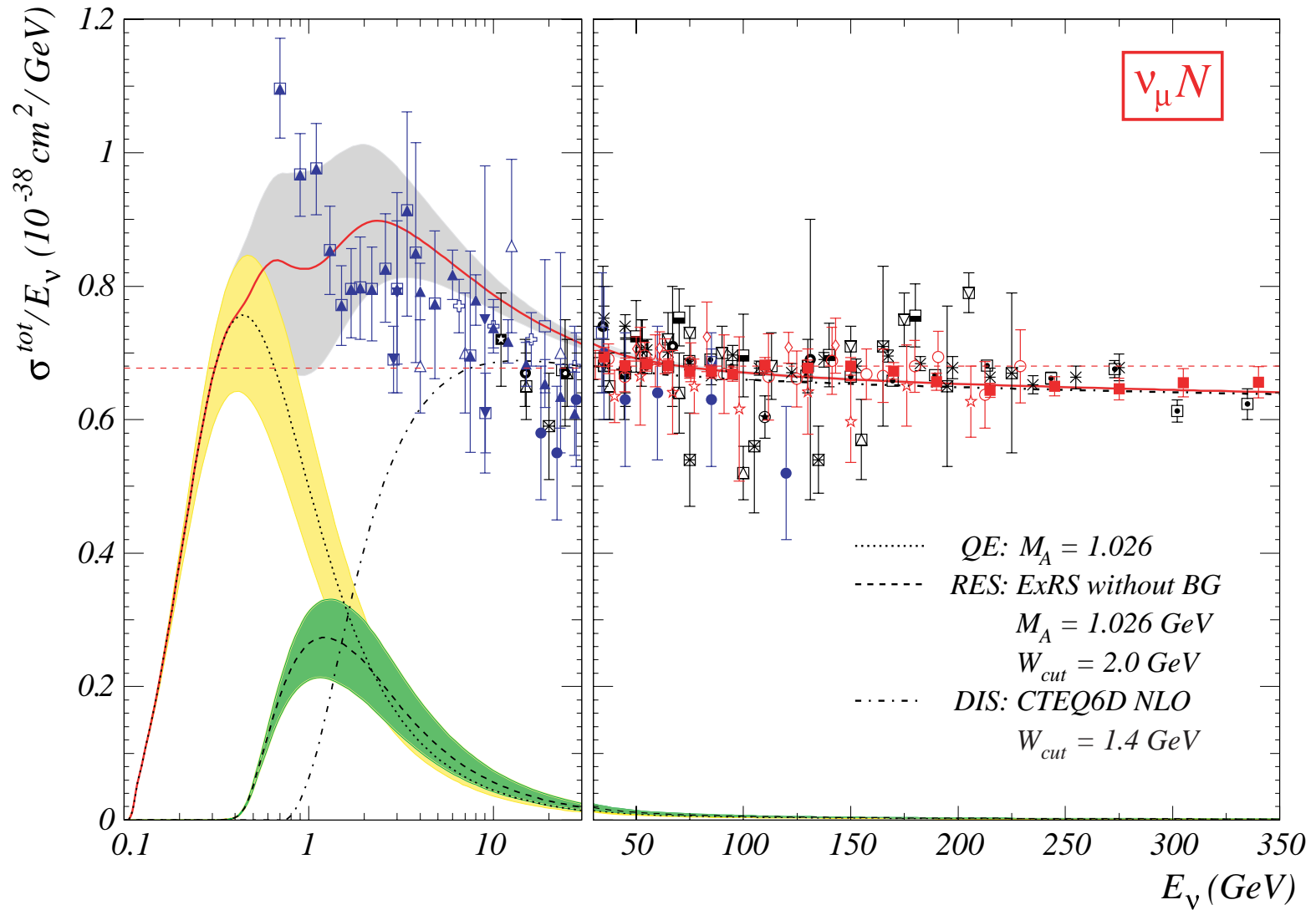
- ✓ the primary vertex should be in the chosen fiducial volume
- ✓ at least two charged tracks at the primary vertex, one of them should be identified as a muon
- ✓ (1) the total visible energy in the event $1 \leq E_\nu \leq 300$ GeV and the reconstructed hadronic mass squared $W \geq 1.4$ GeV^a
- ✓ (2) the total visible energy in the event $40 \leq E_\nu \leq 200$ GeV and the reconstructed hadronic mass squared $W \geq 1.4$ GeV^a
- ✓ (3) the total visible energy in the event $40 \leq E_\nu \leq 200$ GeV^b

Mode	Neutrino		Antineutrino	
	$\langle \sigma_0 \rangle$	N_0	$\langle \sigma_0 \rangle$	N_0
(1)	15.954	968340	4.834	24497
(2)	6.154	370842	2.114	10100
(3)	6.317	380045	2.304	10893

^a A. Bodek and U. K. Yang, "Modeling deep inelastic cross sections in the few GeV region," Nucl. Phys. B (Proc. Suppl.) **112** (2002) 70–76 [arXiv:hep-ex/0203009]; A. Bodek and U. K. Yang, "Higher twist, ξ_w scaling, and effective LO PDFs for lepton scattering in the few GeV region," J. Phys. G **29** (2003) 1899–1906 [arXiv:hep-ex/0210024].

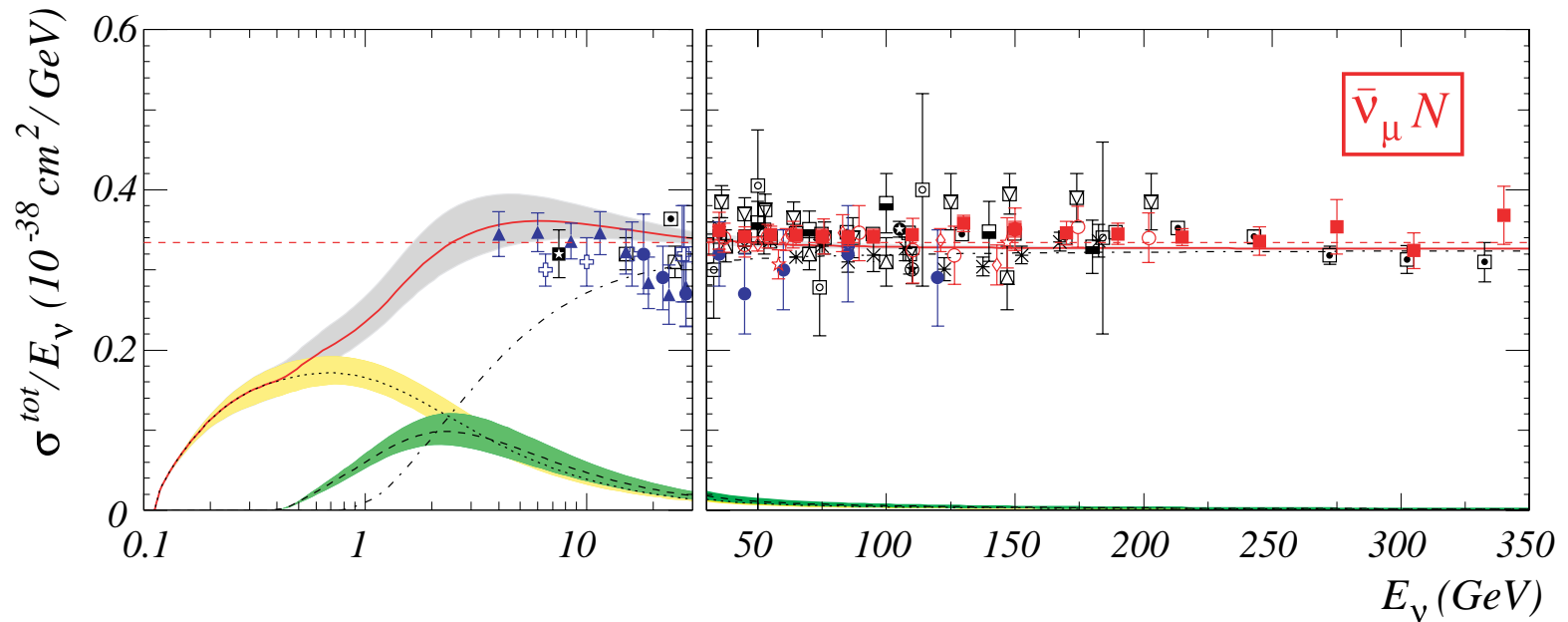
^b S. Eidelman *et al.* (Particle Data Group), Phys. Lett. B **592** (2004) 1–1109

The total ν_μ CC cross section: mixture of QEL, RES and DIS contributions



σ^{tot}/E_ν , for the muon neutrino charged-current total cross section as function of neutrino energy. The straight line is the average value $(0.677 \pm 0.014) \times 10^{-38} \text{ cm}^2/\text{GeV}$.

The total $\bar{\nu}_\mu$ CC cross section: mixture of QEL, RES and DIS contributions



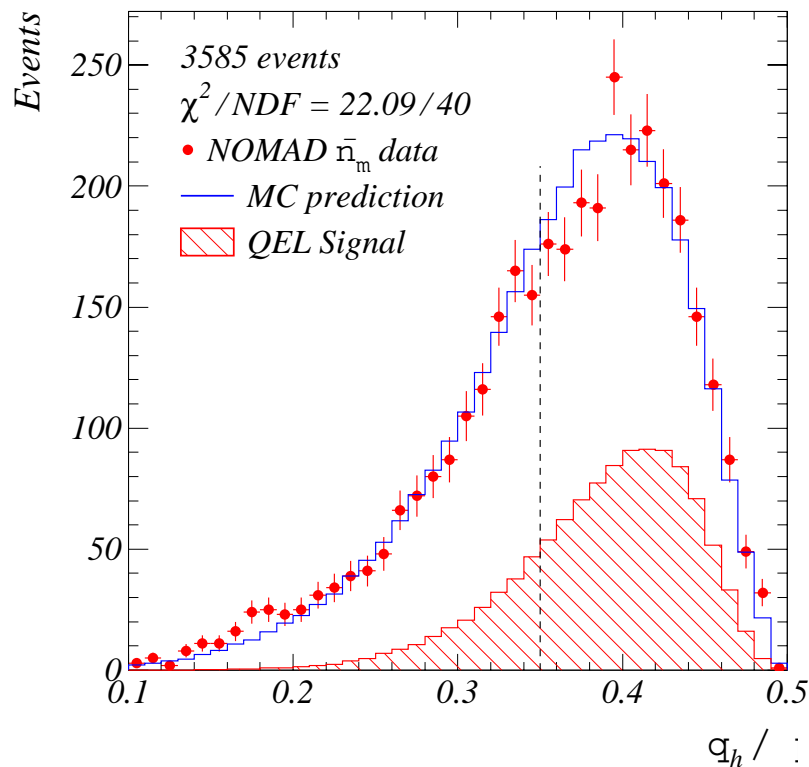
▼ Baltay et al., BNL 1980	■ Seligman, CCFR 1997	⊙ Shotton et al., CDHS 1985
▲ Baker et al., BNL 1982	◻ Naples, NuTeV 2003	◇ Berge et al., CDHS 1987
◻ Barish et al., CCFRR 1981	◻ Colley et al., BEBC 1979	▼ Allaby et al., CHARM 1988
○ MacFarlane et al., CCFRR 1984	◻ Bosetti et al., BEBC 1982	⊗ Jonker et al., CHARM 1981
★ Auchincloss et al., CCFR 1990	◻ Allasia et al., BEBC 1984	◻ Asratyan et al., IHEP-ITEP 1978
● Kitagaki et al., FNAL 1982	▼ Ciampolillo et al., GGM 1979	△ Baranov et al., IHEP SKAT 1979
◻ Taylor et al., HBF 1983	● Morfin et al., GGM 1981	⊕ Vovenko et al., IHEP-ITEP 1979
⊗ Baker et al., FNAL 1983	* Abramowicz et al., CDHS 1983	▲ Anikeev et al., IHEP-JINR 1996

σ^{tot}/E_ν , for the muon antineutrino charged-current total cross section as function of neutrino energy. The straight line is the average value $(0.334 \pm 0.008) \times 10^{-38} \text{ cm}^2/\text{GeV}$.

Signal identification procedure: Antineutrino QEL scattering $\bar{\nu}_\mu p \rightarrow \mu^+ n$

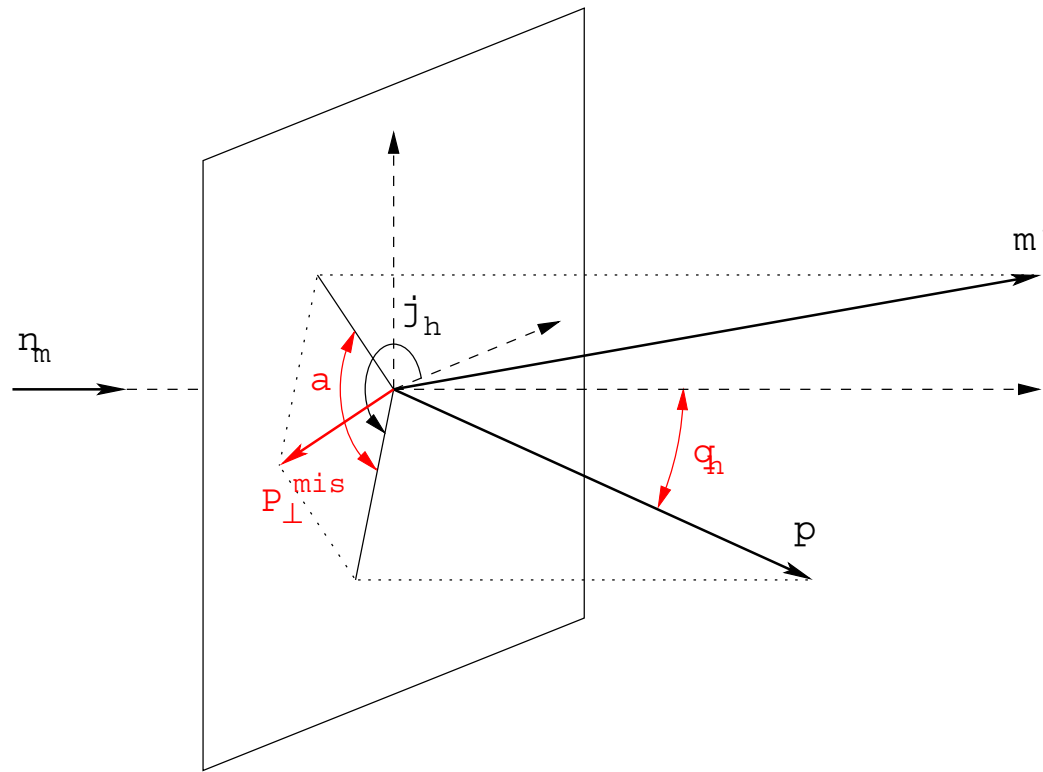
- ✓ reconstructed primary vertex in fiducial volume: $|X, Y| \leq 100$ cm, $5 \leq Z \leq 395$ cm,
- ✓ only one charged track, originated from primary vertex, should be identified as the muon (here we do not take into account neutral tracks and charged tracks, which does not pass quality cuts: $P > 0.3$ GeV and $N_{hits} > 7$)
- ✓ reconstructed kinematical variables:

$$Q^2 = 2M(E_\nu - E_\mu) \quad \Rightarrow \quad E_\nu = \frac{ME_\mu - m_\mu^2/2}{M - E_\mu + P_\mu \cos \theta_\mu} = P_\mu \cos \theta_\mu + P_{pr} \cos \theta_{pr}$$



- reconstructed neutrino energy:
 $3 \leq E_\nu \leq 100$ GeV,
- muon emission angle θ_μ :
 $\theta_\mu/\pi \leq 0.1$
- fake angle θ_h between the proton momentum and the z axis: $0.2 \leq \theta_h/\pi \leq 0.5$,

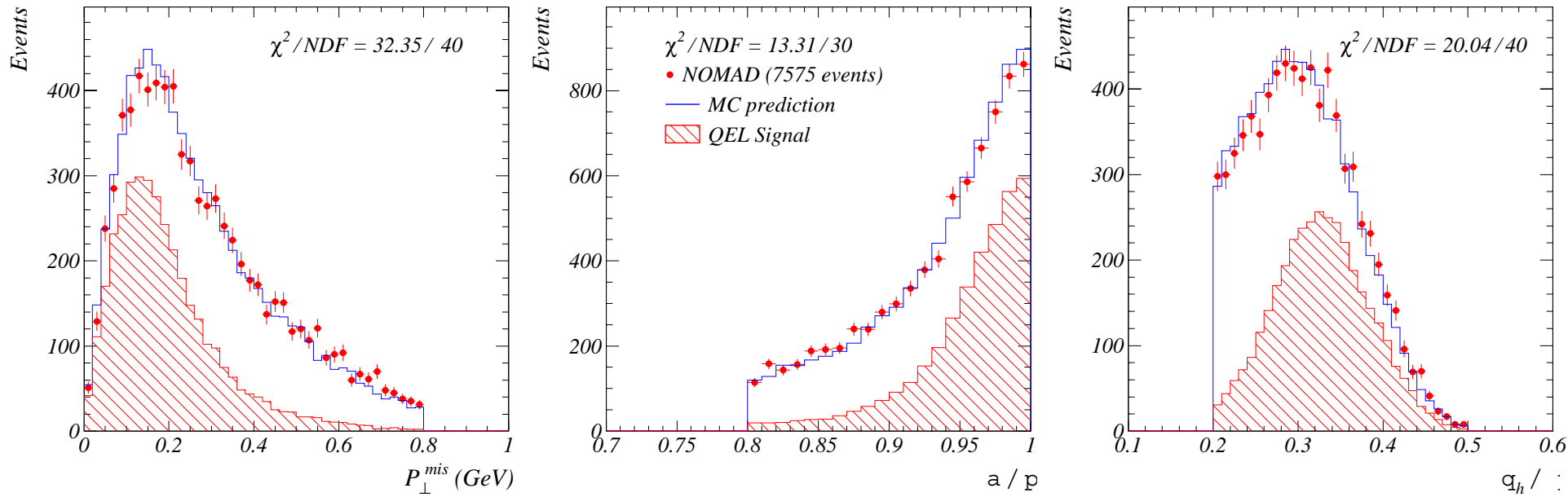
Signal identification procedure: Neutrino QEL scattering $\nu_\mu n \rightarrow \mu^- p$



- $E_\mu = (P_\mu^2 + m_\mu^2)^{1/2}$, $P_\mu = |\vec{k}'|$
- $E_\nu = P_\mu \cos \theta_\mu + P_h \cos \theta_h$
- $Q^2 = 2E_\nu(E_\mu - P_\mu \cos \theta_\mu) - m_\ell^2$

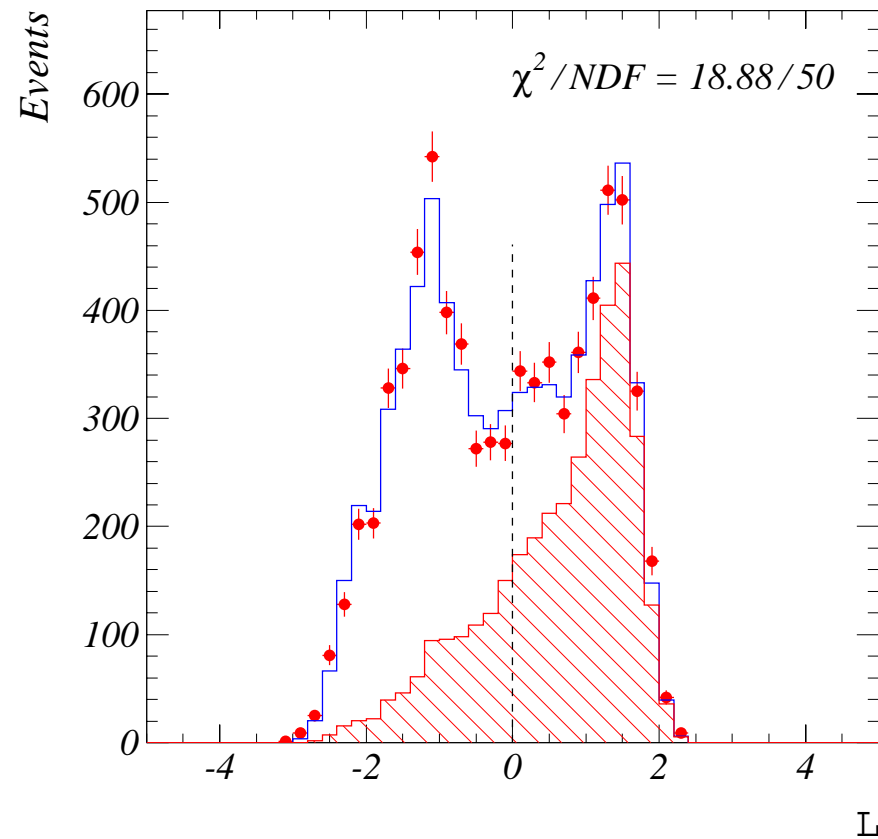
- ✓ proton identification: momentum – range relations,
- ✓ angle α between the transverse components of the charged primary tracks: $0.8 \leq \alpha/\pi \leq 1$,
- ✓ missing transverse momentum $P_\perp^{mis} \leq 0.8$ GeV,
- ✓ angle θ_h between the proton momentum and the z axis: $0.2 \leq \theta_h/\pi \leq 0.5$,
- ✓ Likelihood ratio $\mathcal{L}(\alpha, P_\perp^{mis}, \theta_{pr}) \geq 0$.

Likelihood variables in simulated events and experimental data



Missing transverse momentum P_{\perp}^{mis} , angle α between the transverse components of the charged primary tracks and angle θ_h between the proton momentum and z axis. Distributions for simulated events of different modes (top). Comparison of expected and experimental data distributions (bottom).

Likelihood ratio

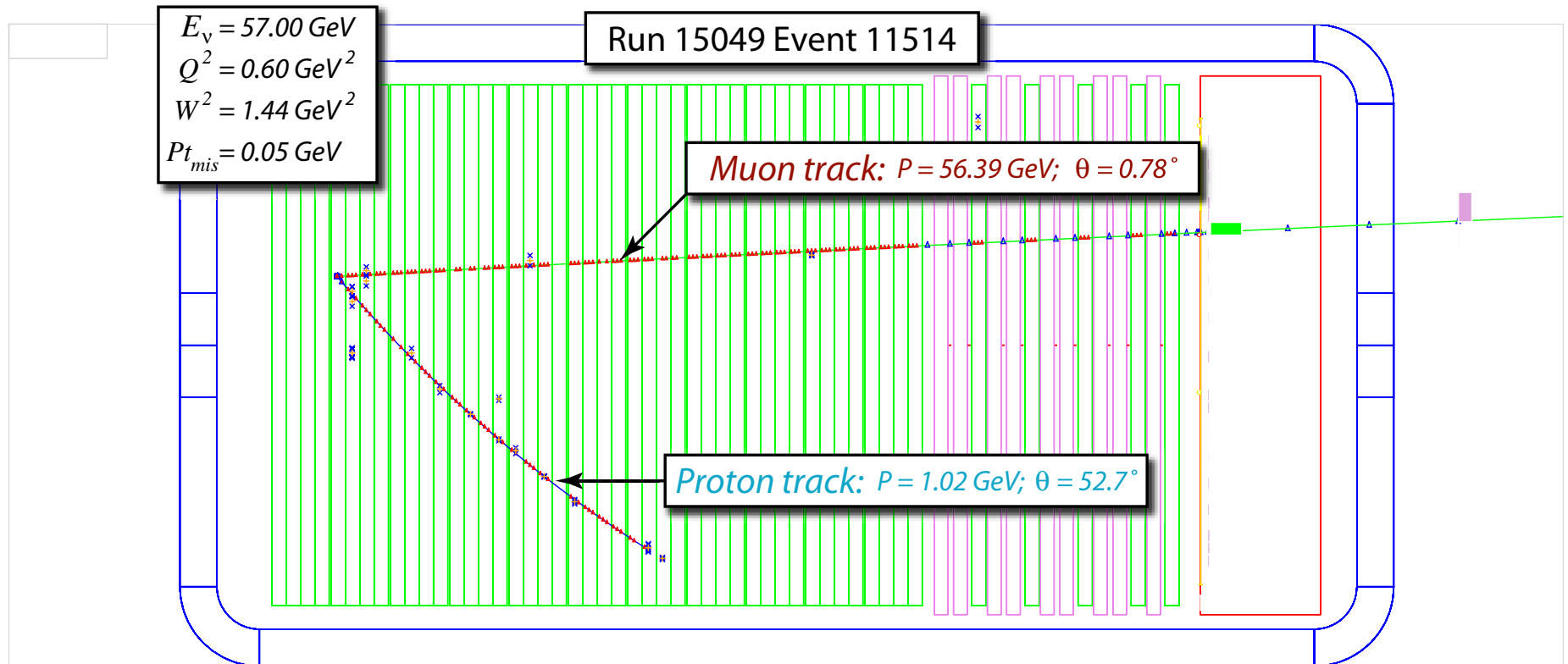


The set of variables $\vec{\ell} = \{P_{\perp}^{mis}, \theta_h, \alpha\}$ can be associated with some likelihood ratio:

$$\mathcal{L} = \ln \frac{P(\vec{\ell} | QEL)}{P(\vec{\ell} | RES)}$$

where $P(\vec{\ell} | QEL)$ and $P(\vec{\ell} | RES)$ are the probabilities for the signal and background events to have kinematic variables $\vec{\ell}$.

View of typical QEL candidate event in NOMAD detector



Typical examples of data events identified as $\nu_\mu + n \rightarrow \mu^- + p$ (run 15049 event 11514). Long track is identified as negatively charged muon, short track is associated with proton.

- **NEUTRINO QEL scattering**

- ✓ We analyse 751.000 ν_μ CC events and identify 14021 QEL candidates with about 49.7% background contamination from the DIS (29.8%) and RES (19.9%) events. Total efficiency of QEL selection is about 34.6%.

- ✓ The measured $\nu_\mu n \rightarrow \mu^- p$ cross section and corresponding axial mass value:

$$\sigma_{qel}^\nu = [0.92 \pm 0.02(stat) \pm 0.06(syst)] \cdot 10^{-38} \text{ cm}^2$$

$$M_A = [1.05 \pm 0.02(stat) \pm 0.06(syst)] \cdot \text{GeV}$$

- **ANTINEUTRINO QEL scattering**

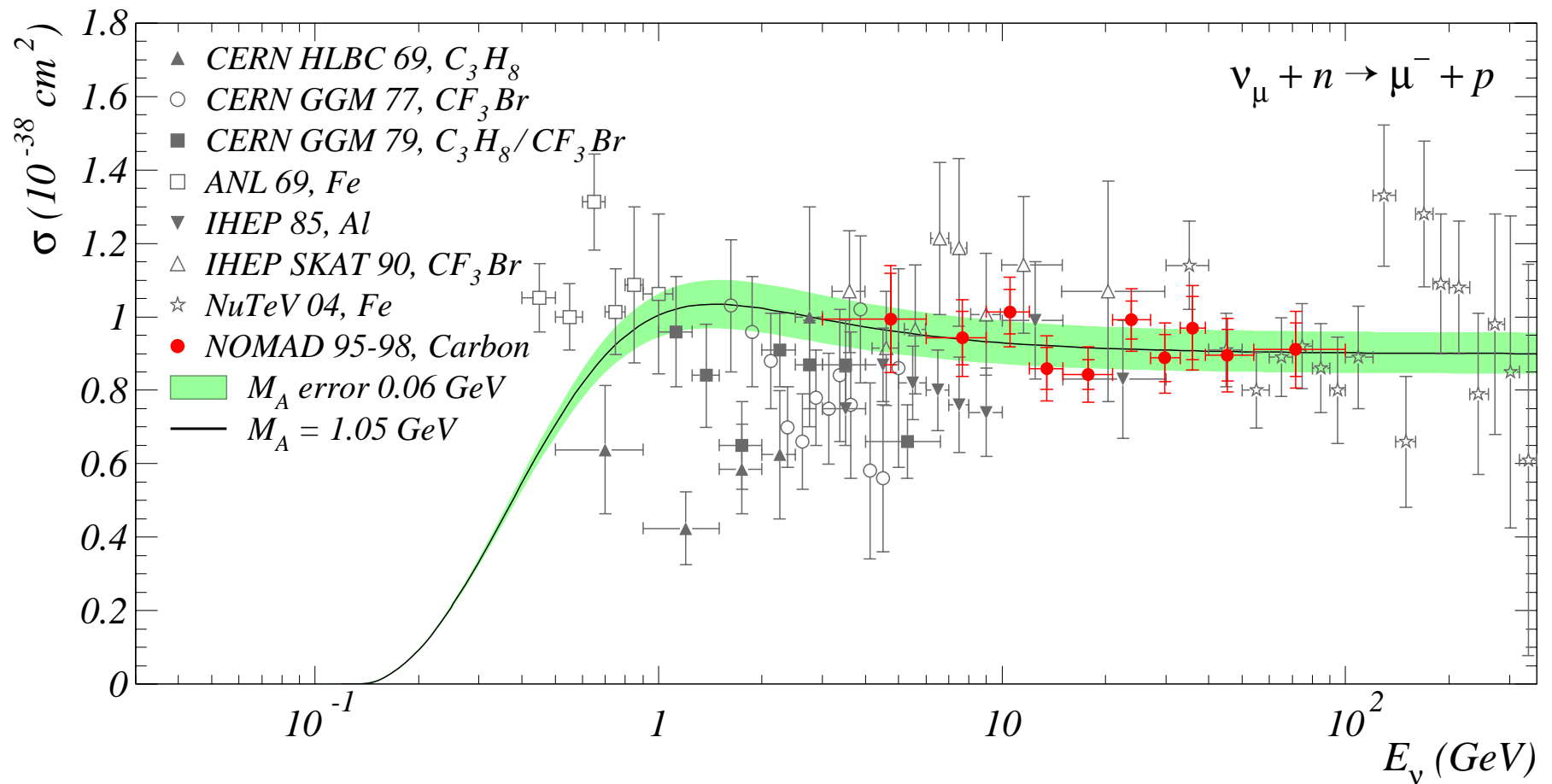
- ✓ We analyse 23.000; $\bar{\nu}_\mu$ CC events and identify 2237 QEL candidates with about 62.0% background contamination from the DIS (33.5%) and RES (28.5%) events. Total efficiency of QEL selection is about 64.4%.

- ✓ The measured $\bar{\nu}_\mu p \rightarrow \mu^+ n$ cross section and corresponding axial mass value:

$$\sigma_{qel}^{\bar{\nu}} = [0.81 \pm 0.05(stat) \pm 0.08(syst)] \cdot 10^{-38} \text{ cm}^2$$

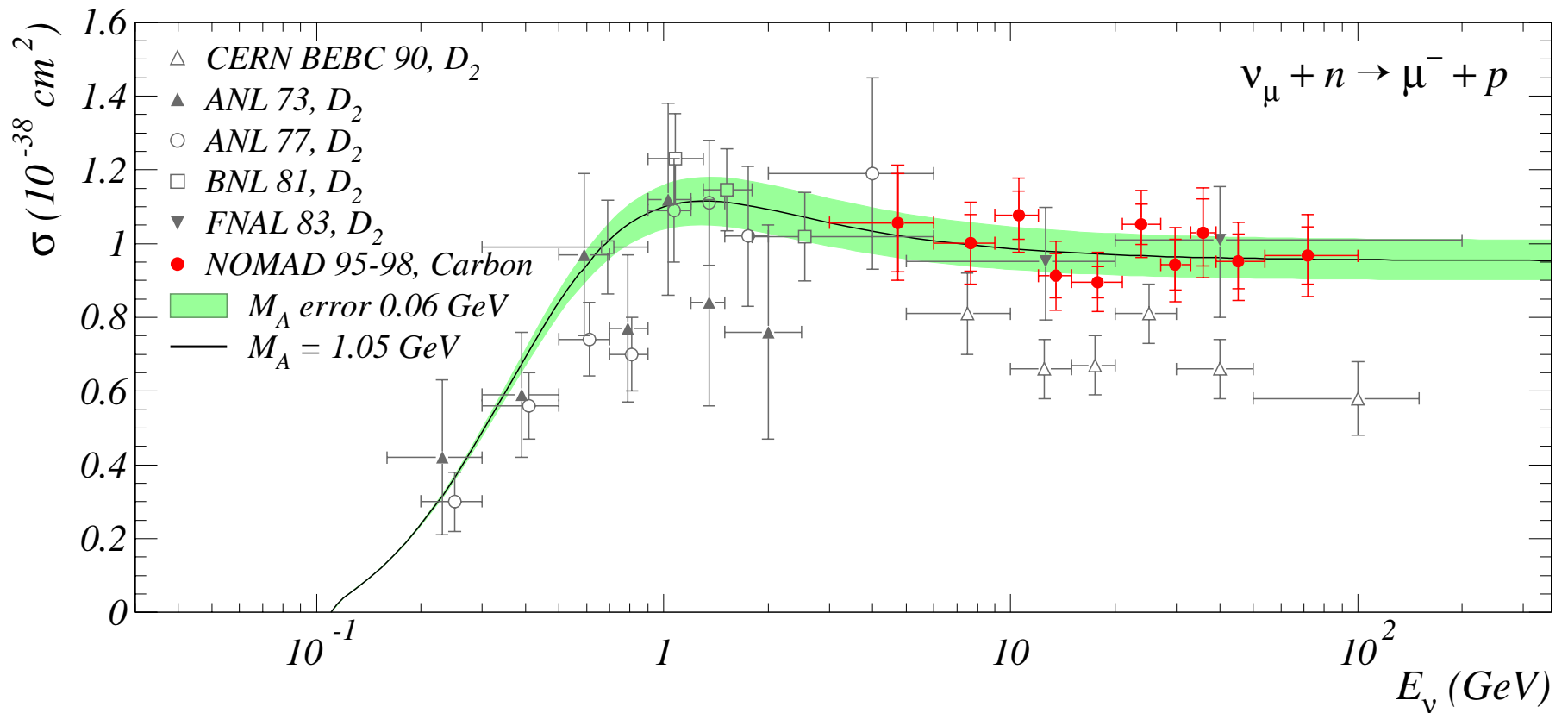
$$M_A = [1.06 \pm 0.07(stat) \pm 0.10(syst)] \cdot \text{GeV}$$

NOMAD results in comparison with previous experimental data



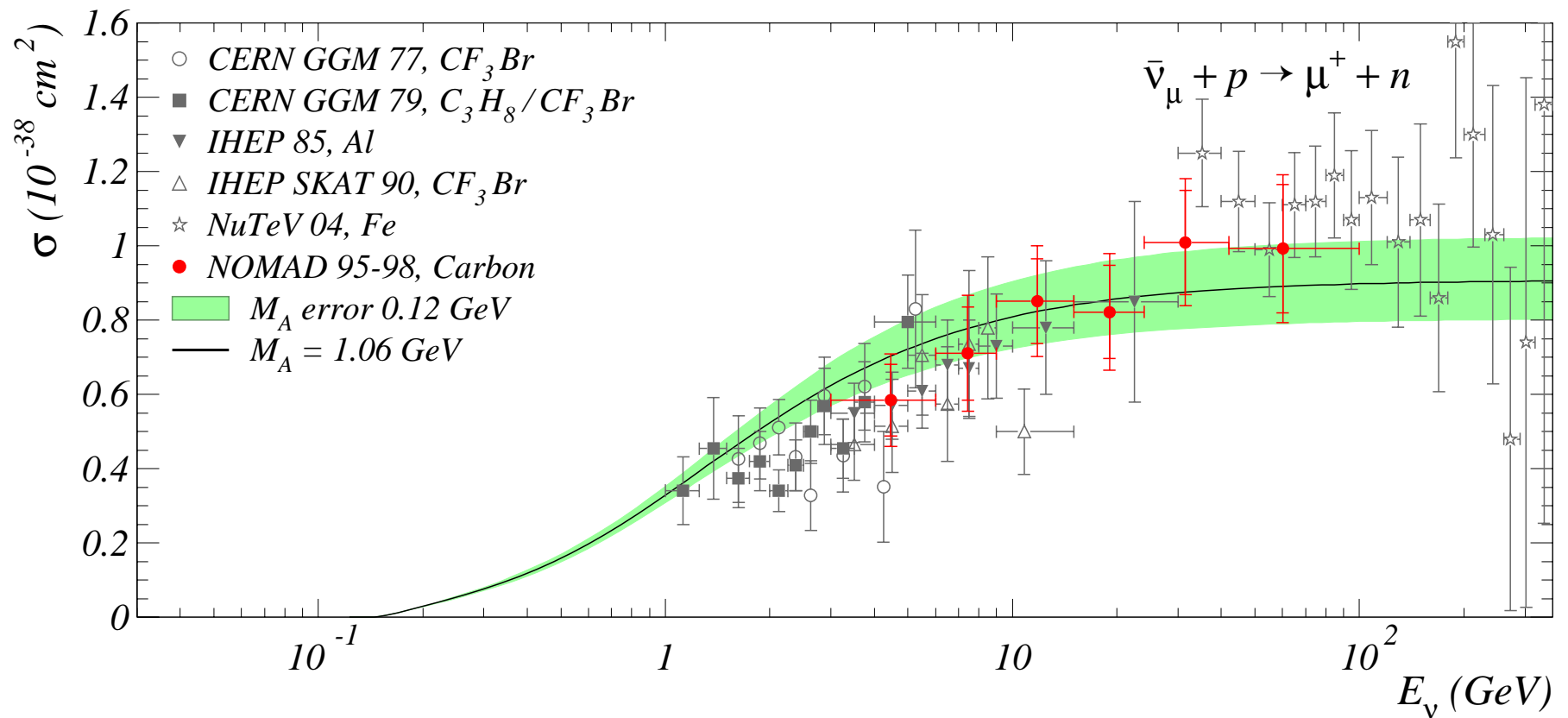
Comparison with previous experimental data extracted from the data on ν_{μ} scattering off heavy nuclei. The solid line and error band corresponds to the M_A value obtained in the NOMAD experiment. Nuclear effects are included into calculations according to the standard relativistic Fermi gas model. The theoretical band corresponds to both statistical and systematical uncertainties.

NOMAD results in comparison with previous experimental data



Comparison with previous experimental data from deuterium filled bubble chambers. The solid line and error band corresponds to the M_A value obtained in the NOMAD experiment. All experimental data are corrected to nuclear effects.

NOMAD results in comparison with previous experimental data



The total cross-section of $\bar{\nu}_\mu p \rightarrow \mu^+ n$ process extracted from the data on $\bar{\nu}_\mu$ scattering off heavy nuclei. Nuclear effects are included into calculations according to the standard relativistic Fermi gas model. Solid line and error band corresponds to the M_A value obtained in the NOMAD experiment.

Systematic uncertainties in QEL cross section

- ✓ (1) QEL Identification procedure. The corresponding errors can be estimated by varying the selection criteria within reasonable limits (likelihood $\mathcal{L} = -2 \div 1.2$ and $\theta_{pr}/\pi = 0.3 \div 0.4$)
- ✓ (2) Uncertainty in the DIS cross-section, used both for normalization and DIS background subtraction. Experimental errors are 2.0% for ν_μ and 2.5% for $\bar{\nu}_\mu$.
- ✓ (3) Uncertainty of the single pion production cross-section. We assume 10% error in $\langle\sigma_{res}\rangle$.
- ✓ (4) Nuclear reinteractions (Intranuclear cascade).
- ✓ (5) Shape of neutrino spectrum.
- ✓ (6) Neutral Current contribution.
- ✓ (7) Muon misidentification.
- ✓ (8) Coherent Diffractive Pion Production ($\nu_\mu + Z \rightarrow \mu^- + Z + \pi^+$)

Source	$\langle\sigma_{qel}\rangle_{\nu_\mu}$	M_A from $\langle\sigma_{qel}\rangle_{\nu_\mu}$	M_A from $d\sigma_\nu/dQ^2$	$\langle\sigma_{qel}\rangle_{\bar{\nu}_\mu}$	M_A from $\langle\sigma_{qel}\rangle_{\bar{\nu}_\mu}$
1	3.2	2.9	2.4	4.3	4.2
2	2.9	2.6	0.2	4.2	4.2
3	4.0	3.6	0.6	7.6	7.4
4	1.7	1.6	6.5	–	–
5	0.2	0.2	0.1	0.9	0.9
6	< 0.1	< 0.1	–	1.1	1.1
7	< 0.1	< 0.1	–	1.0	1.0
8	0.8	0.7	< 0.1	1.1	1.1
total	6.1	5.5	7.0	9.9	9.5

Axial mass M_A measurement from the Q^2 distribution

To extract the axial mass from the Q^2 distribution the experimental data are fit to the theoretical predictions using a traditional χ^2 method:

$$\chi^2(M_A) = \sum_{i=1}^{N_B} \frac{[N_i^{dat} - N_i^{th}(M_A)]^2}{N_i^{dat}}$$

where N_i^{exp} is the number of events in the i -bin of *non-weighted* experimental 2-dimensional $Q^2 \times E_\nu$ distribution, while N_i^{th} is a superposition of the normalized MC background (N^{res} , N^{dis}) and the expected signal:

$$N_i^{th}(M_A) = N_i^{bg} + C \sum_{j=1}^{N_B+1} \varepsilon_{ij}^{qel} \Phi_j \langle \tilde{\sigma}_{qel} \rangle_j$$

$$\text{where } \Phi_i = \int_{E_i}^{E_{i+1}} \Phi(E) dE, \quad \sum_{i=1}^{N_E} \Phi_i = 1$$

$$\langle \tilde{\sigma}_{qel} \rangle_i = \frac{1}{\Phi_i} \int_{\Omega_i} \frac{d\sigma}{dQ^2}(E, Q^2, M_A) \Phi(E) dE dQ^2$$

$$\Phi_i \langle \tilde{\sigma}_{qel} \rangle_i |_{i=N_B+1} = \langle \sigma_{qel} \rangle - \sum_{j=1}^{N_B} \Phi_j \langle \tilde{\sigma}_{qel} \rangle_j$$

Coefficient C can be defined by two ways:

1. the N_i^{th} distribution is normalized to the total number of events in the experimental data:

$$\sum_{i=1}^{N_B} N_i^{th} = \sum_{i=1}^{N_B} N_i^{dat}$$

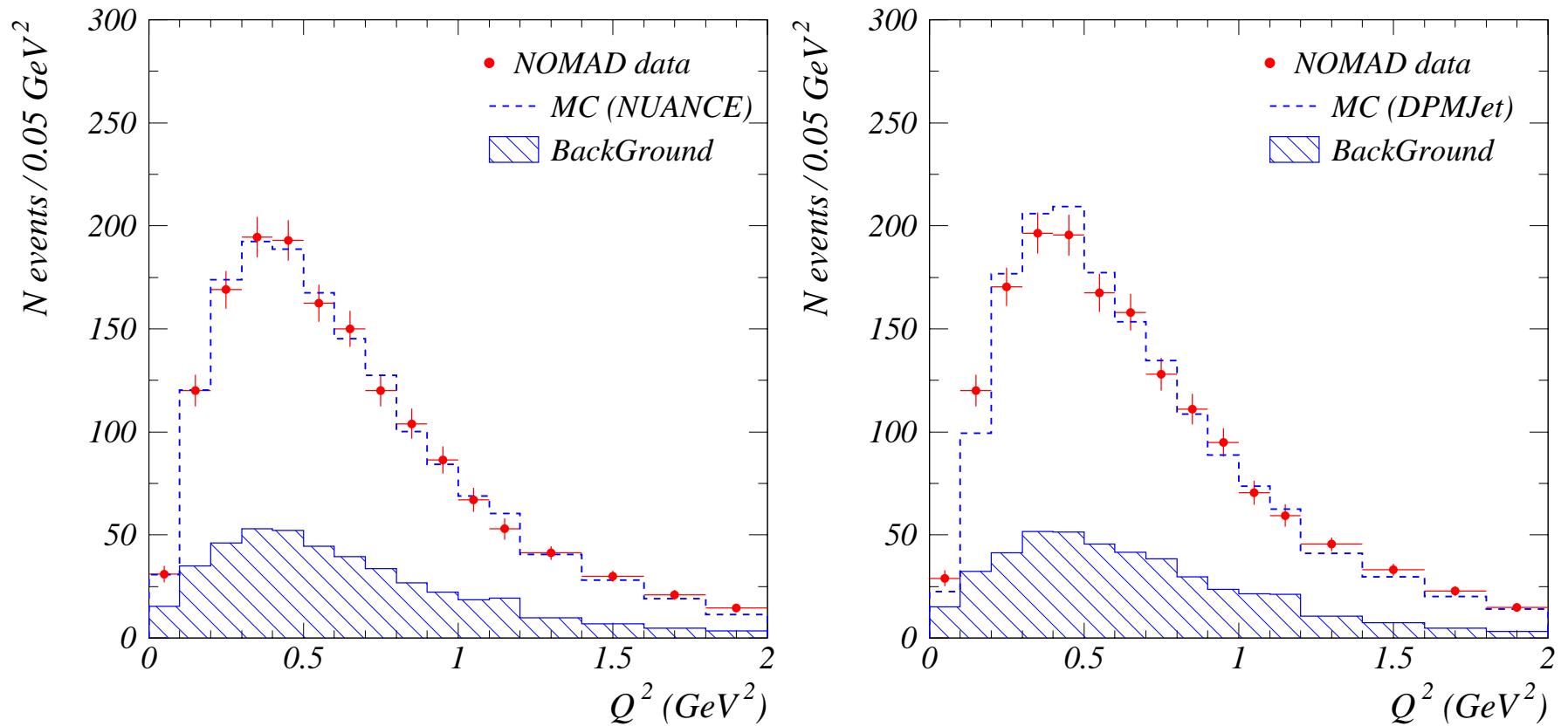
In this case proposed method should be sensitive only to the shape of the distribution but not to the absolute number of identified events (contrary to the M_A measurement from the total QEL cross-section).

2. C is defined by the same way as for the total QEL cross-section measurement, i.e. we use the second process for normalization:

$$C = \frac{N_0}{\Phi_0 \sigma_0}$$

This variant of the fit can be considered as simultaneous fit of the total and differential cross-sections, below we shall refer to it as $\sigma \otimes d\sigma/dQ^2$ fit.

Axial mass M_A measurement from the Q^2 distribution



Q^2 distribution in identified QEL events in MC and experimental data: comparison between DPMJet and NUANCE generators.

$$M_A = 1.07 \pm 0.05 \text{ GeV}$$

Conclusion

- ✓ We performed the most up to date accurate measurement of the $\nu_{\mu}n \rightarrow \mu^{-}p$ cross-section on bounded nucleon. Cross section and corresponding axial mass of the dipole parametrization of the axial form-factor results have the best statistical precision with comparable systematic uncertainties.
- ✓ The experimental data for $\bar{\nu}_{\mu}p \rightarrow \mu^{+}n$ process does not contradict to neutrino data.
- ✓ Obtained results are found to be in good agreement with ones obtained in the previous bubble chamber experiments, but they do not support results, published recently by K2K and MiniBooNE collaborations.